Behavioral/Systems/Cognitive

Dopamine Depletion Impairs Frontostriatal Functional Connectivity during a Set-Shifting Task

Atsuko Nagano-Saito,[1] Marco Leyton,[2] Oury Monchi,[3] Yael K. Goldberg,[1] Yong He,[1] and Alain Dagher[1]

[1]Montreal Neurological Institute and [2]Department of Psychiatry, Faculty of Medicine, McGill University, Montréal, Quebec, Canada H3A 2B4, and [3]Centre de Recherche, Institut Universitaire de Gériatrie de Montréal, Université de Montréal, Montréal, Quebec, Canada H3W 1W5

We investigated the effect of transient dopamine depletion on functional connectivity during performance of the Wisconsin Card Sorting Task. Functional magnetic resonance imaging data were analyzed as a psychophysiological interaction, a statistical method used to identify functional connectivity during experimental manipulations. Nineteen healthy subjects were scanned, double blind, on 2 separate days: once after drinking an amino acid mixture deficient in the dopamine precursors tyrosine and phenylalanine, and once after drinking a nutritionally balanced mixture. In the balanced drink session, statistically significant connectivity between the frontal lobes and striatum was observed during set shifting, and the greater the prefrontostriatal connectivity, the faster the response time after a shift. Neither of these associations were observed after dopamine depletion. Moreover, dopamine depletion also reduced the degree of deactivation in areas normally suppressed during attention-demanding tasks, including the medial prefrontal cortex, posterior cingulate cortex, and hippocampus. Together, these results suggest that functional connectivity between the frontal lobes and basal ganglia during set shifting contributes to more efficient performance and that dopamine modulates this corticostriatal connectivity.

Key words: **dopamine; tyrosine depletion; striatum; prefrontal cortex; fMRI; connectivity; set shifting**

Introduction

Dopamine plays a role in a wide range of cognitive tasks that involve manipulation and monitoring of information in working memory, planning and organization of complex behavior, and flexible shifts in attention. An archetypal example of such a task is the Wisconsin Card Sorting Task (WCST), which requires establishing and then shifting response rules, or task-sets, that entail attending to one specific aspect of a visually presented stimulus. We refer to these types of tasks as frontostriatal because lesion and functional neuroimaging studies implicate the lateral prefrontal cortex (PFC) and striatum in their performance. In animals, dopamine depletion or blockade in PFC or striatum leads to impaired working memory performance (Taghzouti et al., 1985; Sawaguchi and Goldman-Rakic, 1994; Kori et al., 1995; Miyoshi et al., 2002). Patients with Parkinson's disease, who suffer loss of brain dopamine, also show impairments in frontostriatal cognitive function (Lees and Smith, 1983; Taylor et al., 1986; Lange et al., 1992; Owen et al., 1992). Neuroimaging studies have demonstrated impaired activity in the PFC and striatum in Parkinson's disease subjects while they perform various cognitive tasks that depend on working memory (Owen et al., 1998; Dagher et al., 2001; Lewis et al., 2003; Monchi et al., 2004, 2007).

The striatum receives abundant projections from the frontal lobe (Alexander et al., 1986; Middleton and Strick, 2000, 2002). A possible effect of dopamine is to change the connectivity of the corticostriatal thalamocortical loop by enhancing active connections and suppressing inactive ones (Bamford et al., 2004), in a sense increasing the signal-to-noise ratio within the loop. The dopaminergic neurons project close to the corticostriatal glutamatergic synapses (Smith and Bolam, 1990) and are known to modulate corticostriatal connection strength (Bamford et al., 2004). Indeed, in humans, dopamine neurotransmission has an effect on functional connectivity within the corticostriatal thalamic loops (Williams et al., 2002; Honey et al., 2003; Meyer-Lindenberg et al., 2007). The hypothesis of the current study is that enhancement of corticostriatal functional connectivity by dopamine may underpin set shifting and maintenance during the WCST. Corticostriatal modules may do this by biasing attention and responding based on the current task-set.

We previously demonstrated that set shifting in the WCST required simultaneous activation of the PFC and striatum in healthy volunteers (Monchi et al., 2001) and that this activation pattern was deficient in Parkinson's disease patients, possibly indicating impaired frontostriatal connectivity (Monchi et al., 2004). However, cognitive and neuroimaging abnormalities in Parkinson's disease cannot be attributed to dopamine deficiency alone because the disease affects other neurotransmitters (Scatton et al., 1983) and is associated with intrinsic frontal cortical degeneration (Nagano-Saito et al., 2005). We therefore wanted to measure the effect of dopamine depletion on frontostriatal function in the healthy brain using the acute phenylalanine/tyrosine depletion (APTD) technique (Palmour et al., 1998; Leyton et al., 2000).

Received Aug. 28, 2007; revised Feb. 5, 2008; accepted Feb. 18, 2008.

This work was supported by Canadian Institutes of Health Research Grant 144079. We thank Mike Fereirra of the McConnell Brain Imaging Centre for assistance in scanning and analysis.

Correspondence should be addressed to Dr. Alain Dagher, Montreal Neurological Institute, 3801 University Street, Montreal, Quebec, Canada H3A 2B4. E-mail: alain.dagher@mcgill.ca.

DOI:10.1523/JNEUROSCI.3921-07.2008

 0270-6474/08/283697-10$15.00/0

Materials and Methods

Subjects

Nineteen healthy subjects (mean age, 22.6 ± 2.2 years; range, 18–27; seven males; 16 right-handed, two left-handed, one ambidextrous) were recruited for this study. No subject had a history of neurological or psychiatric disorder. Only nonsmokers and social smokers (less than five cigarettes per day) participated. Social smokers were asked to refrain from smoking for at least 24 h before each scan. Drug use, with the exception of occasional marijuana, was an exclusion criterion, and subjects were asked to refrain from using marijuana 1 week before each session. All subjects gave informed consent to the protocol, which was reviewed and approved by the Research Ethics Boards of the Montreal Neurological Institute (MNI) and the "Regroupement Neuroimagerie Quebec" at the Institut Universitaire de Gériatrie de Montréal.

Acute dopamine depletion

It is possible to partially deplete dopamine in healthy volunteers by administering an amino acid drink lacking the dopamine precursors tyrosine and phenylalanine. This treatment transiently decreases dopamine synthesis (Palmour et al., 1998; Leyton et al., 2000) and reduces both baseline dopamine levels and stimulated dopamine release in humans (Montgomery et al., 2003; Leyton et al., 2004). The reduction in dopamine release in the striatum is at least 30%, based on studies in animals (McTavish et al., 1999) and humans (Leyton et al., 2004). The treatment impairs performance on tasks dependent on working memory (Harmer et al., 2001; Gijsman et al., 2002; Harrison et al., 2004). The degree of frontostriatal cognitive impairment correlates with the level of striatal dopamine depletion as measured by positron emission tomography (Mehta et al., 2005).

Subjects were tested twice, on separate days at least 3 d apart. The day before each test session, participants ate a low-protein diet provided by the investigators and fasted from midnight. On the test days, participants arrived at 9:00 A.M. and had blood samples drawn to measure plasma amino acid concentrations (Leyton et al., 2000). After a practice session of the WCST (see below), they ingested one of two amino acid drinks in a randomized, double-blind manner. One drink was a nutritionally balanced 100 g amino acid mixture (BAL), and the other was tyrosine and phenylalanine deficient (APTD) but otherwise identical. Nine subjects received the BAL on the first day, and 10 subjects received APTD first. After ingestion of the amino acid drink, at 10:00 A.M., participants remained awake in a room with relatively neutral videos and reading material available to them before functional magnetic resonance imaging (fMRI) scanning, which started at 2:30 P.M. At the end of the fMRI test session, around 3:30 P.M., participants had a second blood sample drawn to measure plasma amino acid concentration. All female subjects participated while in the follicular phase of their menstrual cycle.

Subjective effects of amino acid drinks were measured with the bipolar Profile of Mood States (POMS) (Lorr et al., 1982) and 10 visual analog scales (Bond and Lader, 1974) at the time of arrival at the laboratory, immediately before the fMRI scan, and after the fMRI scan. These data were analyzed with repeated-measures ANOVA.

Cognitive task

A computerized version of the WCST (Monchi et al., 2001, 2004) was administered using Media Control Function stimulus presentation software (Digivox, Montreal, Quebec, Canada).

At the time of arrival at the laboratory, after blood sampling, subjects were trained on the task for 12 min. Before entering the scanner, they also performed the task for 4 min for additional training. At ~2:00 P.M., subjects were brought to the MRI suite. After a 14 min anatomical scan, the first fMRI run started at 2:30 P.M. During scanning, subjects viewed the computer display via an angled mirror. Throughout this task, four fixed reference cards were present in a row at the top of the screen, displaying one red triangle, two green stars, three yellow crosses, and four blue circles, respectively. On each trial, a new test card was presented in the middle of the screen below the reference cards. Subjects then had to match the test card to one of the reference cards based on the color, shape, or number of the stimuli. Two mouse buttons were used by the subjects to indicate their response with their right index and middle fingers: the left button to move a cursor to point to one of the reference cards and the right button to confirm the selection. After the selection, feedback was presented for 2.4 s: an incorrect match was indicated by darkening the display, whereas a correct trial was signaled by brightening it. After six consecutive correct responses, the matching rule was changed. The rule change resulted in an incorrect match by the subject and negative feedback. Therefore, the receipt of negative feedback signaled the need for a set shift. In addition, there were control trials, during which the test card was identical to one of the four reference cards. On the control trials, subjects were asked to match the test card to the identical reference card. During the scanning session, the subjects performed four types of trials: WCST trials that required matching according to color, shape, or number and control trials. The duration of each matching period depended on the subject's response time (RT).

To study the pattern of activation during the different stages of the WCST, four experimental event periods and two control event periods were defined. (1) Receiving negative feedback (RNF), indicating that a set shift is required, starts immediately after an incorrect selection is made and ends when the next test card is presented. (2) Matching after negative feedback (MNF) starts from the moment the first test card is presented after negative feedback and ends when the subject completes his or her selection. (3) Receiving positive feedback (RPF) starts immediately after a correct selection is made and ends when the next test card is presented. (4) Matching after positive feedback (MPF) starts from the moment a new test card is presented after positive feedback and ends when the subject completes his or her selection. (5) Control feedback (RCF) starts from the moment a selection is made during a control trial and finishes when the next control card is presented. The original brightness of the display is maintained during this period. (6) Control matching (MCF) starts from the moment a new control card is presented and ends when the selection is completed.

Each scanning session contained six functional runs. Within each run, blocks of each of the four trial types (color, shape, number, and the control trials) were presented in random order, with the restriction that no one trial block could be repeated before all four trial types had occurred. In the experimental WCST trial blocks, six correct matching responses in a row had to be completed before a set shift occurred. The control trial blocks consisted of eight trials. Individuals were asked to perform the task continuously during the scanning period, and their responses were recorded by a computer.

fMRI scanning

Subjects were scanned at the Institut Universitaire de Gériatrie de Montréal using a 3T Siemens (Erlangen, Germany) Magnetom Trio MRI scanner. Each scanning session began with a high-resolution, T1-weighted, three-dimensional volume acquisition for anatomical localization (1 mm^3 voxel size). This was followed by acquisitions of echoplanar T2*-weighted images with blood oxygenation level-dependent (BOLD) contrast (echo time, 30 ms; flip angle, 90°). To decrease saturation effects in the orbitofrontal area, phase encoding was performed from the posterior to the anterior direction. Functional images were acquired in six runs in a single session. The volumes were acquired continuously every 2.5 s within each run, and 170 volumes were acquired for each run. Volumes contained 40 slices each of 3.4 mm thickness (matrix size, 64 × 64 pixels; voxel size, 3.4 × 3.4 × 3.4 mm^3). During scanning, a prospective acquisition correction method was applied to reduce errors attributable to head motion (Thesen et al., 2000). Stimulus presentation and scanning were synchronized at the beginning of each run.

fMRI data analysis

Categorical general linear model analysis. First, we identified the brain areas involved in set shifting, set maintenance, and matching using an event-related categorical general linear model (GLM) analysis. The first two frames in each run were discarded. Images from each run were realigned to the third frame of the first run and smoothed using a 6 mm full-width half-maximum isotropic Gaussian kernel.

Activity in the appropriate control period trials was subtracted from that of the different experimental event periods of the color, shape, and number trials combined to generate the following four contrasts for

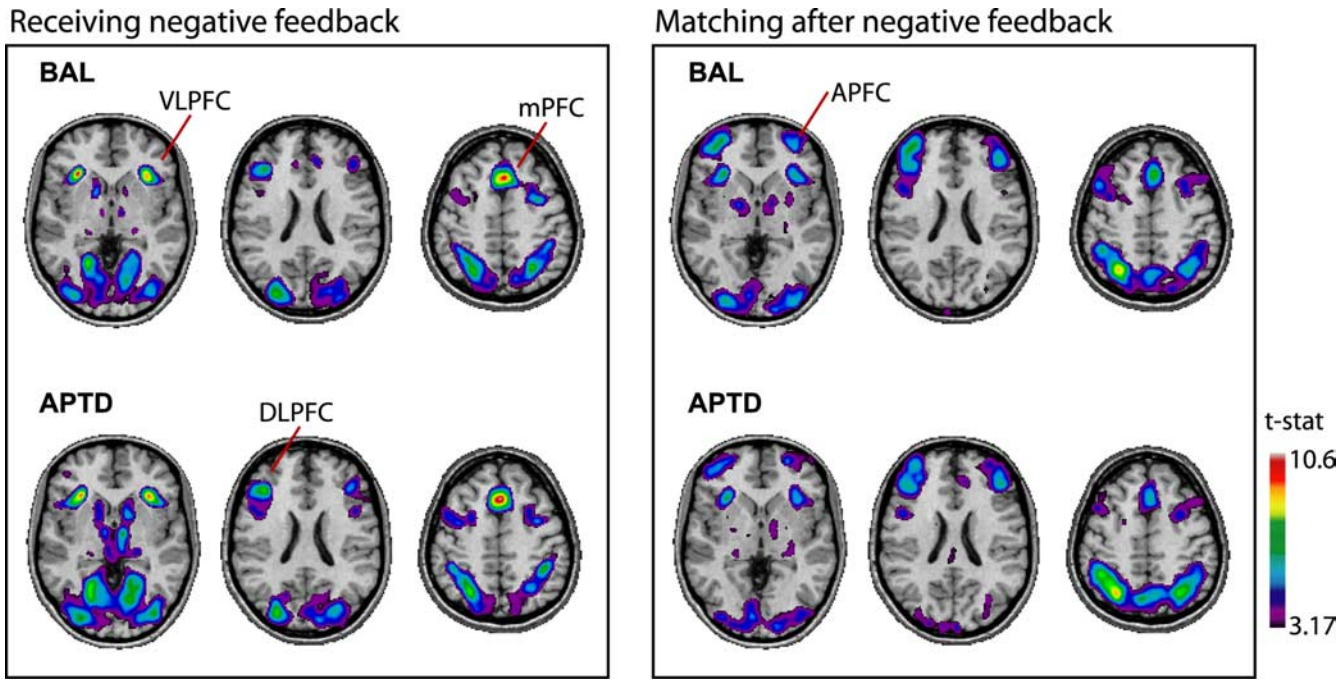

Figure 1. Activation during set shifts. *t*-maps of the contrasts (RNF − RCF) and (MNF − MCF) in the two conditions are shown.

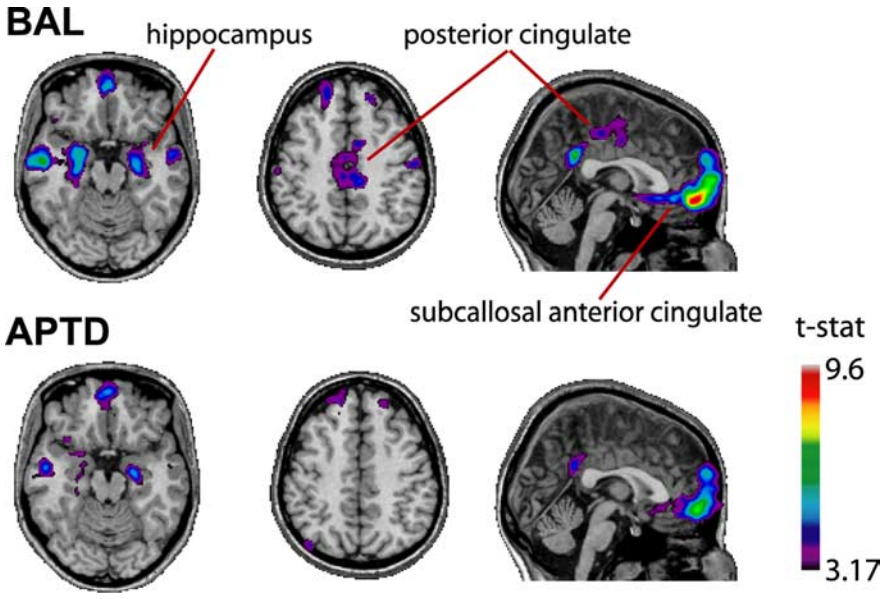

Figure 2. Deactivation during set shifts. Significantly deactivated regions during (RNF − RCF) in BAL and APTD, respectively ($p < 0.001$), are shown.

statistical analysis: (1) RNF in the WCST minus RCF; (2) MNF in the WCST minus MCF; (3) RPF in the WCST minus RCF; and (4) MPF in the WCST minus MCF.

The data analysis was performed using fmristat (Worsley et al., 2002; Worsley, 2005) running in Matlab (The Mathworks, Natick, MA). The fMRI data were first converted to a percentage of the whole volume. The statistical analysis was based on a linear model with correlated errors. The design matrix of the linear model was first convolved with a hemodynamic response function modeled as a difference of two gamma functions (Glover, 1999). Temporal drift was removed by adding a cubic spline in the frame times to the design matrix (one covariate per 2 min of scan time), and spatial drift was removed by adding a covariate in the whole volume average. Slice timing correction was applied. The correlation structure was modeled as an autoregressive process of degree one. At each voxel, the autocorrelation parameter was estimated from the least-squares residuals using the Yule-Walker equations, after a bias correction for correlations induced by the linear model. The autocorrelation parameter was first regularized by spatial smoothing and then used to whiten the data. The linear model was then reestimated using least squares on the whitened data to produce estimates of effects and their SDs at each voxel. The resulting effects and SD images were then linearly transformed into the standard proportional stereotaxic space of the MNI template (ICBM152) using the parameters of the anatomical MRI to template transformation, which were computed using a feature-matching algorithm (Collins et al., 1994).

In a second step, runs, sessions, and subjects were combined using a mixed-effects linear model. A random-effects analysis was performed by first estimating the ratio of the random-effects variance to the fixed-effects variance, then regularizing this ratio by spatial smoothing with a Gaussian filter. The amount of smoothing was chosen to achieve 100 effective degrees of freedom. The variance of the effect was then estimated by the smoothed ratio multiplied by the fixed-effects variance. All peaks that reached $p < 0.05$ corrected for multiple comparisons are reported. Predicted peaks that reached $p < 0.001$ ($t > 3.17$) uncorrected are also reported and identified with an asterisk. A region was predicted if it had been identified in our previous study with this task (Monchi et al., 2001).

Psychophysiological interaction analysis. To investigate how dopamine levels affect functional connectivity during the different cognitive events of the WCST, the BOLD data were submitted to a voxel-based correlation analysis (Friston et al., 1997). The highest peak voxels of each subject in each contrast (RNF − RCF, MNF − MCF, RPF − RCF, MPF − MCF) of the GLM analysis were used as seeds for psychophysiological interaction (PPI) analysis. The voxels of each individual were selected in the bilateral

Table 1. Categorical analysis

			BAL				APTD			
Contrast	Regions		*x*	*y*	*z*	*t* value	*x*	*y*	*z*	*t* value
RNF > RCF[a]	Anterior									
	mPFC	Midline	2	22	48	9.93	2	22	48	10.65
	DLPFC	lt	−38	30	20	6.81	−40	32	20	7.56
			−46	22	28	5.17	−52	24	28	5.78
			−26	10	58	4.78*	−30	10	62	4.45*
		rt	46	32	26	5.12*	40	32	20	5.42
			34	2	50	6.70	34	8	56	5.65
	Posterior PFC	lt	−46	10	32	5.67	−44	10	32	6.58
		rt	40	8	30	5.58	42	8	28	5.46
	VLPFC	lt	−30	26	2	10.42	−30	26	0	9.46
		rt	34	24	0	9.20	34	24	0	9.4
	Posterior									
	Cu (ant), PC	lt	−18	−66	6	7.47	−12	−68	10	6.93
		rt	12	−70	8	6.56	12	−68	8	6.94
	LG	lt	−28	−68	−8	9.54	−32	−66	−10	8.26
		rt	20	−76	−8	8.20	24	−78	−10	7.95
	MOG	lt	−34	−86	8	8.07	−32	−88	12	9.02
		rt	34	−88	8	6.58	38	−84	4	7.40
	PrCu	lt	−24	−74	32	6.22	−28	−72	36	7.75
		rt	28	−72	36	5.48				
	SPL/IPL	lt	−30	−58	48	6.47	−28	−66	46	7.63
		rt	28	−62	50	7.40	42	−44	46	7.44
	Subcortical									
	Caudate	lt	−14	6	0	5.47	−14	14	4	5.00*
		rt	14	8	2	3.97*	14	6	0	5.79
	Thalamus	lt	−8	−12	6	4.86*	−8	−10	6	6.57
		rt	10	−12	8	5.09*	10	−12	4	7.97
RNF < RCF[a]	Midline									
	mOFC	Midline	4	54	−10	−9.65	2	56	−10	−7.29
	mFG/AC	Midline	−6	−8	48	−4.18*				
	CG	Midline	12	−30	46	−4.83*				
	PC	Midline	−2	−50	30	−6.69	−8	−46	36	−4.75*
	Temporal lobe									
	STG	lt	−56	−6	4	−7.52				
	MTG	lt	−46	6	−36	−6.01				
		rt	46	10	−36	−5.47				
	MTL	lt	−24	−14	−22	−7.10				
		rt	28	−4	−24	−6.24	22	−16	−22	−5.61
	Insula	rt	36	4	12	−6.71				
MNF > MCF[b]	Anterior									
	mPFC	Midline	2	24	48	7.02	2	36	36	6.39
	DLPFC	lt	−44	34	24	6.18	−46	34	24	6.00
			−42	32	32	5.99	−48	22	34	5.83
			−30	8	60	5.32	−30	10	62	5.51
		rt	42	36	30	7.01	44	36	24	6.58
			32	14	58	5.12*	34	8	56	5.65
	Posterior PFC	lt	−44	6	32	5.04*	−44	4	32	6.21
		rt					46	6	28	4.49*
	VLPFC	lt	−30	26	−2	6.79	−30	24	−2	6.60
		rt	36	24	−2	6.44	34	26	−4	5.93
	APFC	lt	−38	52	6	7.81	−38	50	16	7.09
		rt	32	56	12	5.92	34	54	14	5.30
			36	54	−8	6.67				
	Posterior									
	Cu (ant), PC	lt	−4	−76	8	5.09*	−8	−78	6	5.29
	PrCu	lt	−28	−72	36	7.75				
		Midline	2	−68	48	5.67	−6	−72	50	6.93
	SPL/IPL	lt	−30	−66	46	9.07	−30	−66	48	9.08
			2	−68	48	5.67	−6	−72	50	6.93
		rt	32	−62	44	6.85	30	−66	50	7.61
	Cu (post)	lt	−24	−95	−8	6.65				
		rt	32	−84	−12	6.12				
	FG	rt	38	−78	−16	6.54	40	−78	−18	7.41
	Subcortical									
	Putamen	lt	−28	2	4	3.41*	−30	4	−2	3.61*
		rt	32	0	2	4.24*				

(*Table continues*.)

Table 1. Continued

Contrast	Regions		BAL x	BAL y	BAL z	BAL t value	APTD x	APTD y	APTD z	APTD t value
	GP	lt	−16	−4	0	4.98*	−12	−10	10	4.57*
		rt	14	−2	2	4.74*	14	−4	6	4.99*
	Cerebellum	lt	−10	−72	−32	7.47	−4	−78	−24	7.06
			−30	−64	−34	6.84	−50	−64	−16	6.51
		rt	8	−78	−26	6.99	8	−78	−26	6.89
			40	−70	−30	7.03	40	−76	−16	7.30
MNF < MCF[b]	Midline									
	mOFC	Midline	0	56	−10	−6.26	−6	50	−6	−6.23
	mFL/AC	Midline	2	−18	50	−4.70*				
	CG	Midline					2	−26	52	−5.76
	Temporal Lobe									
	STG	rt	72	−24	14	−5.25				
	MTL	lt	−22	−14	−16	−6.60				
		rt	26	−16	−16	−6.03				
RPF > RCF[c]	Anterior									
	Posterior PFC	lt	−40	2	36	4.36*				
	Posterior									
	Cu (ant), PC	rt	8	−72	8	7.38	8	−72	10	7.34
	MOG	rt	42	−80	−14	5.28				
	SPL/IPL	lt	−26	−68	36	4.58*				
		rt	36	−60	48	5.13				
	Cu (post)	rt	14	−98	0	5.29				
RPF < RCF[c]	None									
MPF > MCF[d]	Anterior									
	mPFC						0	16	50	5.62
	DLPFC	lt					−40	32	24	5.51
		rt					−28	4	62	5.36
	VLPFC	lt					−30	22	4	5.63
	Posterior									
	Cu (ant), PC	lt					−10	−78	6	5.32
	PrCu	lt					8	−72	52	5.51
		Midline					−8	−72	50	5.67
	SPL/IPL	lt	−26	−68	42	5.54	−30	−68	52	7.56
		Midline					−8	−72	50	5.67
		rt					32	−66	52	5.88
	FG	lt	−38	−74	−14	5.69				
		rt					40	−74	−14	6.45
MPF < MCF[d]	Temporal lobe									
	STG	lt	−68	−22	14	−5.33				

lt, Left; rt, right; ant, anterior; post, posterior; AC, anterior cingulate gyrus; CG, cingulate gyrus; Cu, cuneus; FG, fusiform gyrus; GP, globus pallidus; IPL, inferior parietal lobe; LG, lingual gyrus; MFG, middle frontal gyrus; mFG, medial frontal gyrus; mOFC, medial orbitofrontal cortex; MOG, middle occipital gyrus; MTG, middle temporal gyrus; MTL, medial temporal lobe; PC, posterior cingulate gyrus; PrCu, precuneus; Put, putamen; SPL, superior parietal lobe; STG, superior temporal gyrus.

[a]Receiving negative feedback minus control feedback (corrected $p < 0.05$; $t > 5.13$; *significant at uncorrected $p < 0.001$ with a priori hypothesis).

[b]Matching after negative feedback minus matching after control feedback (corrected $p < 0.05$; $t > 5.13$; *significant at uncorrected $p < 0.001$ with a priori hypothesis).

[c]Receiving positive feedback minus control feedback (corrected $p < 0.05$; $t > 5.13$; *significant at uncorrected $p < 0.001$ with a priori hypothesis).

[d]Matching after positive feedback minus matching after control feedback (corrected $p < 0.05$; $t > 5.13$).

Table 2. Significant connectivity between the frontal lobes and the brain regions in the BAL session

Seeds	Regions	x	y	z	t value	p value of cluster extent
mPFC	Putamen	26	10	8	3.75	0.018
Left APFC	Putamen	30	10	8	4.80	0.001
Right APFC	Putamen	−28	6	2	3.87	0.032
Left DLPFC	Putamen	−20	10	4	4.86	<0.001
	Putamen	24	14	8	4.79	0.001
	Caudate	−14	−6	22	4.60	0.003
Right DLPFC	Putamen	30	12	10	4.18	0.026
	Caudate	18	6	22	4.65	<0.001
Left VLPFC	Putamen	30	10	6	4.04	0.001
	Caudate	18	16	8	4.24	0.002
Right VLPFC	Caudate	−8	0	10	5.46	<0.001
	Caudate	8	10	6	5.08	<0.001

There were no significant peaks in the APTD session, even when lowering the threshold to $p < 0.001$, uncorrected. p values given are corrected for multiple comparisons based on the size of the whole striatum search volume.

dorsolateral PFC (DLPFC; Brodmann's areas 9, 46, 9/46), ventrolateral PFC (VLPFC; Brodmann's area 47/12), anterior PFC (APFC), and medial PFC (mPFC). From this peak voxel and the six adjacent voxels (effectively creating a small volume of interest), the BOLD signal time courses of each 7 min run were extracted. An interaction product was then created between this averaged time course and the WCST events. To determine functional connectivity modulated by cognitive events, a brain-wide search for voxels where BOLD signal covaried significantly with this interaction term was performed, using the event contrasts as confounds and correcting for slice timing differences. The equation used was as follows:

$$\mathbf{y}_i = x_k \times \mathbf{g}_p \times \mathbf{b}_1 + \mathbf{x}_k \times \mathbf{b}_2 + \mathbf{g}_p \times \mathbf{b}_3 + \mathbf{G} \times \mathbf{b}_4 + \varepsilon_i,$$

where $\mathbf{y}_i$ is the BOLD time course at voxel i, $\mathbf{x}_k$ is the time course at the seed area, $\mathbf{g}_p$ is the task events vector, $\mathbf{G}$ is a general confound term that includes signal drift, $\mathbf{b}$ is the parameter estimates, and ε is the error. The GLM then tests for the effect of the first parameter.

Using a random-effects analysis across subjects, we estimated connectivity between each of the seeds and whole brain, within condition (BAL

and APTD separately) and between conditions (comparison between BAL and APTD). Based on our hypothesis that dopamine acts to increase the connectivity between activated areas in PFC and the striatum during a set shift, all peaks located in the striatum that reached $p \leq 0.05$ ($t > 3.97$) corrected are reported. Peaks that reached $p \leq 0.001$ ($t > 3.17$) uncorrected are also reported and appropriately identified.

Correlation between results of PPI and RT. We hypothesized that if frontostriatal connectivity facilitated set shifting, there should be a correlation with performance. The extensive WCST training before the test sessions led to minimal errors, but RTs varied more substantially. Given this, a correlation analysis was performed between frontostriatal connectivity score during set shifting (RNF − RCF) and the RT difference between MNF and MCF for each individual (Sternberg, 1966) (i.e., the RT for the first match after a set shift). Because the left DLPFC exhibited the greatest functional connectivity with striatum in the PPI, we determined the frontostriatal connectivity score from the connectivity map for the (RNF − RCF) period with the seed in the left DLPFC. First, we segmented each subject's brain to generate a mask of the basal ganglia (BG) consisting of the caudate, putamen, nucleus accumbens, and globus pallidus in MNI space (Chakravarty et al., 2005). We calculated the summed *t* value over all connected voxels in the BG with the left DLPFC (defined as all voxels with $t > 1.67$ corresponding to $p < 0.05$ uncorrected) for each subject for each scanning session to obtain a measure of frontostriatal connectivity. We then performed Pearson's correlation on these connectivity scores and the RT difference between MNF and MCF for each individual (two-tailed *p* values are reported). Because we found a significant result with this analysis, we generated a connectivity *t*-map with a seed in the left DLPFC using RT difference as a covariate.

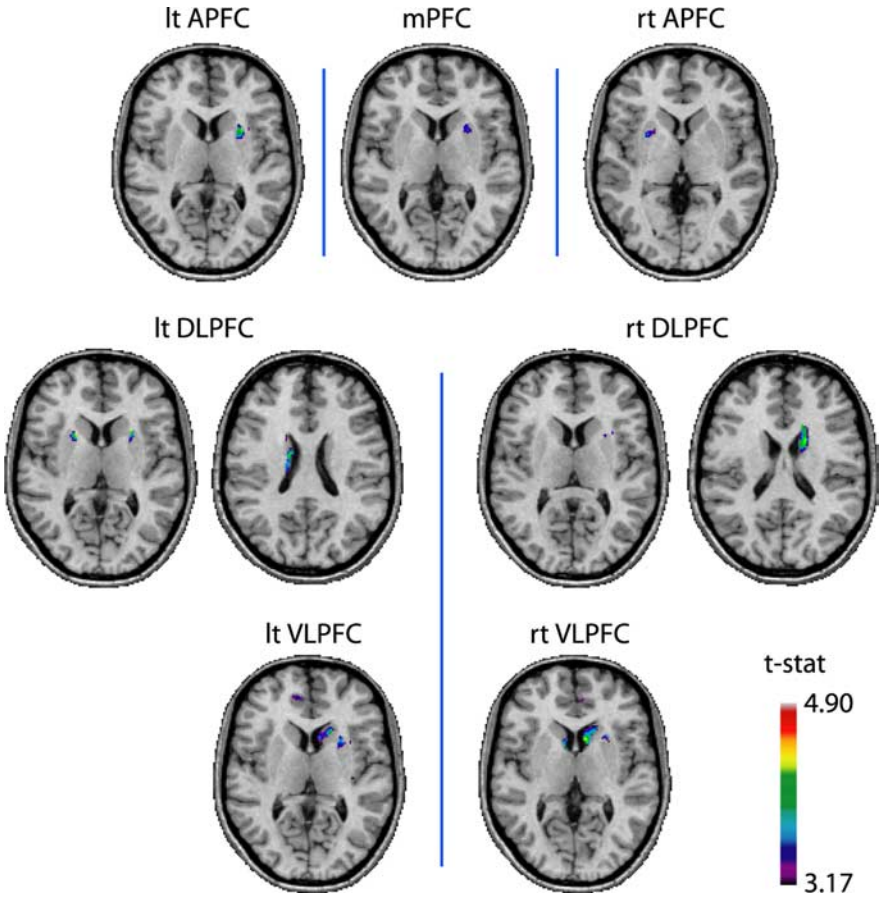

Figure 3. Prefrontostriatal functional connectivity. Significantly connected regions in the BAL condition using the PPI analysis are shown. There were no significant correlations in the APTD session. lt, Left; rt, right.

Results

Plasma amino acid levels

Morning tyrosine levels were 58.2 ± 12.9 and 54.8 ± 11.0 μmol/L on BAL and APTD days, respectively. After fMRI scanning, they were 130.0 ± 34.3 and 13.3 ± 6.0 μmol/L, respectively. For phenylalanine, the morning levels were 54.3 ± 4.5 and 54.6 ± 5.5 μmol/L for BAL and APTD, respectively, and 96.3 ± 37.8 and 14.9 ± 6.6 μmol/L after the fMRI sessions. Repeated-measures ANOVA indicated a significant condition difference between BAL and APTD ($F = 220.0$, $p < 0.001$; $F = 68.0$, $p < 0.001$) and a condition by time interaction ($F = 202.5$, $p < 0.001$; $F = 81.1$, $p < 0.001$) for tyrosine and phenylalanine, respectively. The tyrosine/large neutral amino acid ratio, a measure of brain tyrosine availability, was unchanged during the BAL session (mean and SD: 0.118 ± 0.016 before drinking the solution, 0.109 ± 0.042 after scanning; 7% change; $p = 0.41$) but reduced significantly after APTD (0.116 ± 0.015 and 0.013 ± 0.007; 90% reduction; $p < 0.0001$).

Behavioral results

The mean RT for MNF, MPF, and MCF were 1876 ± 403, 1615 ± 436, and 1511 ± 506 ms during the BAL session and 2011 ± 700, 1710 ± 526, and 1550 ± 546 ms during the APTD session. Two-way, repeated-measures ANOVA showed a significant difference in the RT for the different matching trials MNF, MPF, and MCF ($F = 45.028$; $p < 0.001$). There was a trend toward a difference between the APTD and BAL conditions ($F = 4.071$; $p = 0.059$). All RTs tended to be longer in APTD than in BAL.

The average rates of perseveration errors were 0.9 ± 0.8 and 1.0 ± 1.0%, and non-perseveration errors were 1.3 ± 0.8 and 1.6 ± 1.0%, for the BAL and APTD conditions, respectively. Two-way, repeated-measures ANOVA showed no significant difference between the conditions ($F = 0.435$; $p = 0.52$). There was no significant effect of drink on any of the mood scores, but there was a trend toward lower scores on the Elated–Depressed measure of the POMS in the APTD condition ($p = 0.09$). This was attributable to lower scores (less elated) after the end of the scanning session only.

Table 3. Areas with greater frontostriatal connectivity (from the PPI analysis) in BAL than APTD after receiving negative feedback ($p < 0.001$; $t > 3.17$)

Seeds	Regions	*x*	*y*	*z*	*t* value
Left APFC	Putamen	32	12	8	3.47
Left DLPFC	Putamen	−30	10	10	3.59
	Putamen	22	10	8	3.34
	Caudate	−16	−8	26	3.26
Right VLPFC	Caudate	6	6	10	3.57

Image analysis

Categorical analysis

The results are shown in Table 1 and Figures 1 and 2. The activated and deactivated regions observed during the task were sim-

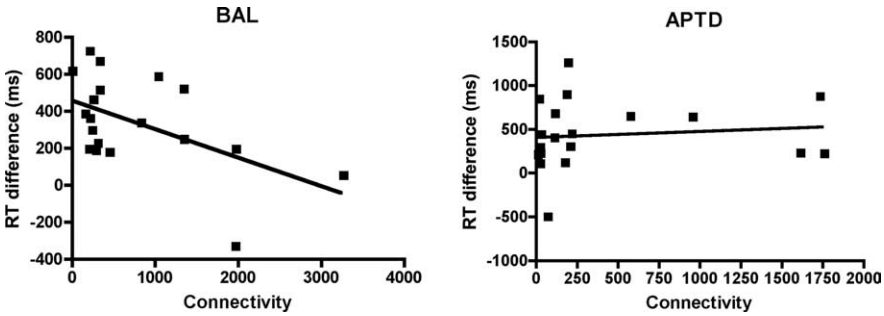

Figure 4. Effect of prefrontostriatal connectivity on RT. Plots of connectivity score between the left DLPFC and the BG during the contrast (RNF − RCF) and RT difference between MNF and MCF. The correlation is significant in the BAL session ($p = 0.02$) but not in the APTD session ($p = 0.67$). TPD, Tyrosine and phenylalanine deficient drink session.

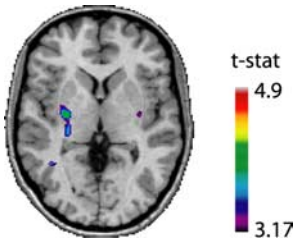

Figure 5. Connectivity between DLPFC and posterior putamen. Significantly functionally correlated regions with the left DLPFC in BAL, using the RT difference (MNF − MCF) as a covariate ($p < 0.001$). Greater functional connectivity between DLPFC and bilateral posterior putamen correlated with greater RT reduction.

ilar to those in our previous report (Monchi et al., 2001). We also observed previously unreported activation in the APFC (Brodmann's area 10) during (MNF − MCF) in this study.

For the main contrasts of interest: receiving negative feedback (RNF − RCF) and matching after negative feedback (MNF − MCF), the activation patterns were similar in BAL and APTD (Fig. 1). While receiving negative feedback, there was robust activation of structures belonging to the cognitive corticostriatal loop, including DLPFC, VLPFC, APFC, posterior parietal cortex, striatum, and thalamus, for both the BAL and APTD conditions. The *t*-maps comparing the two conditions disclosed slightly greater activation in thalamus for the (RNF − RCF) contrast in APTD with a peak of $x = 8$, $y = -20$, $z = 4$, and $t = 3.59$.

Deactivation was observed mainly in the midline and the temporal lobe. In the (RNF − RCF) contrast, the deactivation was greater in BAL than in APTD (Table 1, Fig. 2), and the *t*-maps comparing the two conditions showed slightly greater deactivation in the region of the basal forebrain and subcallosal anterior cingulate gyrus (peak $x = 0$, $y = 0$, $z = -4$, $t = 3.76$) for the BAL condition. There was more extensive deactivation in the medial temporal lobe and posterior cingulate in BAL than APTD (Table 1, Fig. 2).

For the set maintenance contrasts, (RPF − RCF) and (MPF − MCF) (Table 1), activation appeared generally greater in BAL with the contrast of (RPF − RCF) and in APTD with the contrast of (MPF − MCF), but no significant difference was observed at the threshold of $p < 0.05$ corrected.

PPI

At the threshold of $p < 0.05$ corrected, 10 significant connectivities with the frontal lobes were observed in the BG in BAL (Table 2), and none were observed in APTD. Lowering the threshold to $p < 0.001$ uncorrected revealed significantly connected regions in two other striatal regions in the BAL condition but still none in the APTD condition (Table 2, Fig. 3). These statistical peaks were observed only in the contrast of (RNF − RCF), indicating that the period after negative feedback was associated with increased frontostriatal connectivity. The direct comparison between BAL and APTD identified significantly greater connectivity between the PFC and several regions in the BG during BAL at the threshold of $p < 0.001$ uncorrected (Table 3).

Correlation analyses

There was a significant negative correlation between the scores of DLPFC–BG connectivity and the RT difference (MNF − MCF) during the BAL test session ($r = -0.53$; $p = 0.02$) (Fig. 4) but not during the APTD test session ($r = 0.10$; $p = 0.67$). The correlation differed significantly between the two conditions ($t = 1.76$; $p = 0.048$). The statistical parametric map of the correlation analysis using the RT difference as a covariate disclosed significant connectivity of the left DLPFC with the bilateral posterior putamen ($x = -32$, $y = -10$, $z = -2$, $t = -4.09$ on the left and $x = 36$, $y = -10$, $z = -6$, $t = -3.79$ on the right) in BAL (Fig. 5). The direct comparison between BAL and APTD identified significantly greater connectivity between the left DLPFC and the bilateral posterior putamen, with RT difference as a covariate, in BAL at the threshold of $p < 0.001$ uncorrected ($x = -26$, $y = -14$, $z = 4$, $t = -3.20$ on the left and $x = 36$, $y = -8$, $z = -2$, $t = -3.31$ on the right).

Discussion

We used fMRI and APTD to show that reducing dopamine levels caused widespread impairments in frontostriatal functional connectivity as well as increased RTs in a set-shifting task.

Previous neuroimaging studies had suggested that dopamine deficiency in Parkinson's disease led to abnormalities in corticostriatal interaction during frontal lobe tasks (Owen et al., 1998; Dagher et al., 2001). More specifically, those prefrontal areas that appeared to participate in the task as part of a corticostriatal network displayed impaired activation, along with the caudate or putamen, whereas prefrontal areas that appeared to be involved independently of the striatum displayed normal or excessive activation (Monchi et al., 2004, 2007). Our previous studies using the WCST had suggested that coactivation of PFC and striatum was important for efficient planning and execution of a set shift (Monchi et al., 2001) and deficient in Parkinson's disease (Monchi et al., 2004).

In the current study, we found that, although dopamine depletion did not prevent activation of prefrontal and striatal regions during set shifting as seen in Parkinson's disease, it eliminated the functional connectivity between these regions. We found extensive functional connectivity between the activated voxels in the mPFC, APFC, DLPFC, VLPFC, and anterior striatum while receiving negative feedback only in the BAL condition. This indicates that corticostriatal connectivity is under dopaminergic control and is particularly important when set shifting. This is consistent with the clinical observation that, even at an early stage, Parkinson's disease patients are impaired at prefrontal tasks, including the WCST (Gotham et al., 1988). Moreover, in the BAL condition, higher functional connectivity during set shifting correlated with lower RTs during the first match after a set shift, suggesting that connectivity plays a role in establishing the task set to improve performance. Dopamine depletion also disrupted the relationship between connectivity and RT (Fig. 4).

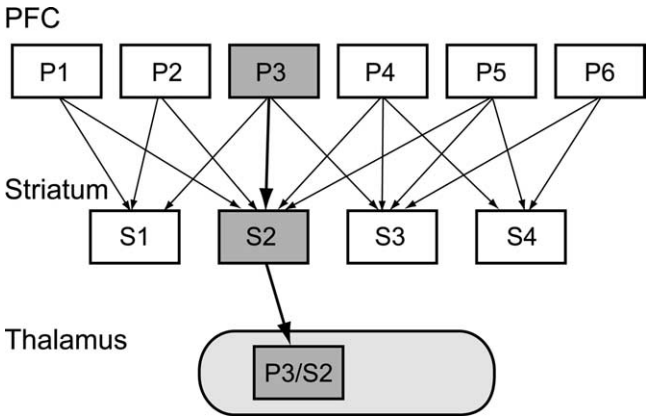

Figure 6. Corticostriatal information flow. This model, adapted from Bar-Gad et al. (2000) and Monchi et al. (2000), explains how data reduction in the frontostriatal system may lead to functional connectivity detected by fMRI. The P_i represent different PFC units, and the S_i represent their targets in striatum. In this case, each P–S connection might represent a different matching rule for the WCST. Assume that P3 and S2 are functionally connected for the current task. If dopamine acts to enhance P3–S2 while suppressing the other P–S2 connections, then both of these effects will increase the correlation between activity in P3 and S2. This action of dopamine could be described as focusing of neuronal activity (Mink, 1996) or as dimensionality reduction in the information encoded by the different PFC modules (Bar-Gad et al., 2000). In any case, it would manifest as enhanced point-to-point corticostriatal functional connectivity detected by fMRI.

Every frontal peak examined showed significant connectivity with the striatum (Table 2), but the connected region in the caudate or putamen differed with the seed voxels. The VLPFC was functionally connected with the caudate head, which is in line with our previous WCST studies (Monchi et al., 2001, 2004) and with a meta-analysis of striatal functional connectivity (Postuma and Dagher, 2006). The DLPFC was functionally connected with the anterior putamen and dorsal caudate body. The APFC was functionally connected with the anterior putamen. In all cases, therefore, prefrontal regions exhibited functional connectivity with portions of the associative, or cognitive, striatum (Parent, 1990), consistent with a role in establishing and switching the matching rules.

Of all frontal regions, the left DLPFC exhibited the greatest functional connectivity with striatum, in terms of spatial extent and statistical significance. This supports the suggestion that a general role for the DLPFC is to establish a set of responses suitable for a given task (Nathaniel-James and Frith, 2002). Indeed, activation of the left DLPFC is consistently observed during a wide variety of high-level cognitive tasks (Duncan and Owen, 2000). We therefore focused on the connectivity of left DLPFC to the striatum to investigate its role in the WCST. The DLPFC–striatum connectivity score was correlated with faster RTs while matching after a set shift, an association that was seen in the BAL condition only. After negative feedback, subjects need to select a new matching rule, implying the need to access the previous rule, and then to match the target card according to the new rule. Connectivity between DLPFC and striatum, under dopaminergic control, seems to support these sequential steps. These results are consistent with the predictions of neural network models in which dopamine-dependent corticostriatal signaling acts to improve RTs by setting a lower decision threshold for action (Lo and Wang, 2006). Establishing a response set involves a similar biasing of responses toward particular stimulus features, which is likely to depend on the focusing of neuronal activity (Mink, 1996). Bar-Gad and Bergman have proposed that the cortico-BG system performs this by a form of data reduction that is akin to principal component analysis (Bar-Gad et al., 2000). This results in extraction of relevant information from cortical activity, yielding a simplified response set leading to more efficient responding (Fig. 6). In the case of the WCST, this would entail focusing on the currently relevant dimension, say color, while ignoring the other two, shape and number. These authors also suggest that this process of data reduction (Bar-Gad et al., 2000) and rule selection (Leblois et al., 2006) is under dopamine control. One supporting piece of evidence is that dopamine depletion leads to a loss of uncorrelation among BG outputs (Pessiglione et al., 2005), implying that the data reduction mechanism is disrupted. Our results add to these models by showing that dopamine depletion also disrupts cortico-BG functional connectivity during set shifting, possibly indicating a reduction in cortical influence on BG outputs. If this is true, correlation of BG outputs during dopamine depletion could represent intrinsic BG activity with the cortical influence removed or lessened. Simultaneous cortical and striatal recordings in mice confirm that, when striatal dopamine is experimentally reduced, corticostriatal neurons have less influence on the firing of striatal neurons (Costa et al., 2006). It should be noted that this last study demonstrated that striatal dopamine depletion affected the correlation between cortical and striatal firing without reducing the overall amount of cortical activity, consistent with our current results: we found that prefrontal and striatal activation peaks were equally prominent in both conditions, but they became uncorrelated during dopamine depletion. More recently, Meyer-Lindenberg et al. (2007) found that the genotype of DARPP-32 (dopamine- and cAMP-regulated phosphoprotein-32), a key regulator of the dopamine second-messenger pathway expressed mainly in striatal dopamine neurons, predicted both frontostriatal connectivity and cognitive performance, including the WCST, in healthy humans.

Although the main prefrontostriatal connectivity analysis yielded peaks in the associative striatum, the analysis that used the RT difference as a covariate identified connectivity between the DLPFC and posterior (motor) putamen (Fig. 5). Again, this was only seen in the BAL condition. It is tempting to speculate that this functional connectivity between PFC and motor striatum indicates information transfer from a cognitive set-shift neural network to a motor neural network for movement. In support of this proposal, patients with Parkinson's disease have been reported to require longer switching cost for RT tasks (Hayes et al., 1998; Cools et al., 2001), especially in the L-dopa off states (Shook et al., 2005), whereas in healthy subjects, administration of a dopamine D_2 antagonist slowed RT on a set-shifting task (Mehta et al., 2004).

However, in Parkinson's disease patients, L-dopa, a dopamine precursor, has not always improved WCST performance (Gotham et al., 1988; Owen et al., 1993; Kulisevsky et al., 1996). This may reflect the fact that, in Parkinson's disease, there may be chronic effects of dopamine deficiency, as well as cortical degeneration (Nagano-Saito et al., 2005) and loss of other neurotransmitters beside dopamine (Scatton et al., 1983). Another possibility, however, is that dopaminergic stimulation has different effects on different individuals depending on their baseline dopamine function and may actually worsen performance in some patients (Mattay et al., 2003; Cools et al., 2007). Indeed, both set-shifting performance and its response to dopaminergic medication vary among Parkinson's disease patients (Williams-Gray et al., 2008).

Another finding in this study was that dopamine levels influ-

enced deactivation in the mPFC and subgenual anterior cingulate, posterior cingulate, and medial temporal lobe (Table 1). There was greater and more extensive deactivation in the BAL condition in these regions while receiving negative feedback (Fig. 2) and while matching after negative feedback. The mPFC, posterior cingulated, and hippocampus are often deactivated during cognitively demanding tasks (Greicius et al., 2003), and the degree of suppression correlates with task difficulty measures, such as working memory load (Esposito et al., 2006), suggesting that deactivation plays a role in task performance. These areas form a network of functionally connected regions that display high activity at rest (Greicius et al., 2003). The posterior cingulate and medial temporal lobe are anatomically (Vogt et al., 1992) and functionally (Greicius et al., 2003) connected and are involved in episodic memory retrieval (Maguire and Mummery, 1999). Suppression of these areas may be necessary to limit interference during certain working memory tasks, in which memory of previous trials could interfere with current trials. The effect of dopamine depletion on deactivation described here is consistent with our previous findings in Parkinson's disease. While performing the Tower of London task, patients demonstrated impaired activation of the striatum along with impaired deactivation of the hippocampus (Dagher et al., 2001). We proposed that suppression of hippocampal activity was useful for performing frontostriatal tasks, such as the Tower of London or the WCST, and that the inability to properly suppress episodic memory function contributed to impaired performance in Parkinson's disease. Indeed, there is considerable evidence that striatum and hippocampus can interfere with each other during learning tasks (Packard et al., 1989; Poldrack et al., 2001). Our current study confirms that dopamine plays a role in suppression of the hippocampus and posterior cingulate during tasks that engage the frontostriatal system. It is not known, however, how dopamine affects suppression of the episodic memory network, nor how this suppression and frontostriatal activation are linked.

In summary, during set shifting, there was increased functional connectivity between PFC and striatum, as well as deactivation of medial frontal, posterior cingulate, and hippocampal areas, and both of these phenomena were disrupted by transiently reducing dopamine levels. This provides a possible mechanism for frontal lobe cognitive impairment in Parkinson's disease and other conditions associated with dopaminergic abnormalities.

References

Alexander GE, DeLong MR, Strick PL (1986) Parallel organization of functionally segregated circuits linking basal ganglia and cortex. Annu Rev Neurosci 9:357–381.

Bamford NS, Zhang H, Schmitz Y, Wu NP, Cepeda C, Levine MS, Schmauss C, Zakharenko SS, Zablow L, Sulzer D (2004) Heterosynaptic dopamine neurotransmission selects sets of corticostriatal terminals. Neuron 42:653–663.

Bar-Gad I, Havazelet-Heimer G, Goldberg JA, Ruppin E, Bergman H (2000) Reinforcement-driven dimensionality reduction—a model for information processing in the basal ganglia. J Basic Clin Physiol Pharmacol 11:305–320.

Bond A, Lader M (1974) The use of analog scales in rating subjective feelings. Br J Med Psychol 47:211–218.

Chakravarty MM, Sadikot AF, Germann J, Bertrand G, Collins DL (2005) Anatomical and electrophysiological validation of an atlas for neurosurgical planning. Med Image Comput Comput Assist Interv Int Conf Med Image Comput Comput Assist Interv 8:394–401.

Collins DL, Neelin P, Peters TM, Evans AC (1994) Automatic 3D intersubject registration of MR volumetric data in standardized Talairach space. J Comput Assist Tomogr 18:192–205.

Cools R, Barker RA, Sahakian BJ, Robbins TW (2001) Mechanisms of cognitive set flexibility in Parkinson's disease. Brain 124:2503–2512.

Cools R, Lewis SJ, Clark L, Barker RA, Robbins TW (2007) L-DOPA disrupts activity in the nucleus accumbens during reversal learning in Parkinson's disease. Neuropsychopharmacology 32:180–189.

Costa RM, Lin SC, Sotnikova TD, Cyr M, Gainetdinov RR, Caron MG, Nicolelis MA (2006) Rapid alterations in corticostriatal ensemble coordination during acute dopamine-dependent motor dysfunction. Neuron 52:359–369.

Dagher A, Owen AM, Boecker H, Brooks DJ (2001) The role of the striatum and hippocampus in planning: a PET activation study in Parkinson's disease. Brain 124:1020–1032.

Duncan J, Owen AM (2000) Common regions of the human frontal lobe recruited by diverse cognitive demands. Trends Neurosci 23:475–483.

Esposito F, Bertolino A, Scarabino T, Latorre V, Blasi G, Popolizio T, Tedeschi G, Cirillo S, Goebel R, Di Salle F (2006) Independent component model of the default-mode brain function: assessing the impact of active thinking. Brain Res Bull 70:263–269.

Friston KJ, Buechel C, Fink GR, Morris J, Rolls E, Dolan RJ (1997) Psychophysiological and modulatory interactions in neuroimaging. NeuroImage 6:218–229.

Gijsman HJ, Scarna A, Harmer CJ, McTavish SB, Odontiadis J, Cowen PJ, Goodwin GM (2002) A dose-finding study on the effects of branch chain amino acids on surrogate markers of brain dopamine function. Psychopharmacology (Berl) 160:192–197.

Glover GH (1999) Deconvolution of impulse response in event-related BOLD fMRI. NeuroImage 9:416–429.

Gotham AM, Brown RG, Marsden CD (1988) "Frontal" cognitive function in patients with Parkinson's disease "on" and "off" levodopa. Brain 111:299–321.

Greicius MD, Krasnow B, Reiss AL, Menon V (2003) Functional connectivity in the resting brain: a network analysis of the default mode hypothesis. Proc Natl Acad Sci USA 100:253–258.

Harmer CJ, McTavish SF, Clark L, Goodwin GM, Cowen PJ (2001) Tyrosine depletion attenuates dopamine function in healthy volunteers. Psychopharmacology (Berl) 154:105–111.

Harrison BJ, Olver JS, Norman TR, Burrows GD, Wesnes KA, Nathan PJ (2004) Selective effects of acute serotonin and catecholamine depletion on memory in healthy women. J Psychopharmacol 18:32–40.

Hayes AE, Davidson MC, Keele SW, Rafal RD (1998) Toward a functional analysis of the basal ganglia. J Cogn Neurosci 10:178–198.

Honey GD, Suckling J, Zelaya F, Long C, Routledge C, Jackson S, Ng V, Fletcher PC, Williams SC, Brown J, Bullmore ET (2003) Dopaminergic drug effects on physiological connectivity in a human cortico-striato-thalamic system. Brain 126:1767–1781.

Kori A, Miyashita N, Kato M, Hikosaka O, Usui S, Matsumura M (1995) Eye movements in monkeys with local dopamine depletion in the caudate nucleus. II. Deficits in voluntary saccades. J Neurosci 15:928–941.

Kulisevsky J, Avila A, Barbanoj M, Antonijoan R, Berthier ML, Gironell A (1996) Acute effects of levodopa on neuropsychological performance in stable and fluctuating Parkinson's disease patients at different levodopa plasma levels. Brain 119:2121–2132.

Lange KW, Robbins TW, Marsden CD, James M, Owen AM, Paul GM (1992) L-dopa withdrawal in Parkinson's disease selectively impairs cognitive performance in tests sensitive to frontal lobe dysfunction. Psychopharmacology (Berl) 107:394–404.

Leblois A, Boraud T, Meissner W, Bergman H, Hansel D (2006) Competition between feedback loops underlies normal and pathological dynamics in the basal ganglia. J Neurosci 26:3567–3583.

Lees AJ, Smith E (1983) Cognitive deficits in the early stages of Parkinson's disease. Brain 106:257–270.

Lewis SJ, Dove A, Robbins TW, Barker RA, Owen AM (2003) Cognitive impairments in early Parkinson's disease are accompanied by reductions in activity in frontostriatal neural circuitry. J Neurosci 23:6351–6356.

Leyton M, Young SN, Pihl RO, Etezadi S, Lauze C, Blier P, Baker GB, Benkelfat C (2000) Effects on mood of acute phenylalanine/tyrosine depletion in healthy women. Neuropsychopharmacology 22:52–63.

Leyton M, Dagher A, Boileau I, Casey K, Baker GB, Diksic M, Gunn R, Young SN, Benkelfat C (2004) Decreasing amphetamine-induced dopamine release by acute phenylalanine/tyrosine depletion: a PET/[11C]raclopride study in healthy men. Neuropsychopharmacology 29:427–432.

Lo CC, Wang XJ (2006) Cortico-basal ganglia circuit mechanism for a decision threshold in reaction time tasks. Nat Neurosci 9:956–963.

Lorr M, McNair DM, Fisher SU (1982) Evidence for bipolar mood states. J Pers Assess 46:432–436.

Maguire EA, Mummery CJ (1999) Differential modulation of a common memory retrieval network revealed by positron emission tomography. Hippocampus 9:54–61.

Mattay VS, Goldberg TE, Fera F, Hariri AR, Tessitore A, Egan MF, et al. (2003) Catechol *O*-methyltransferase val158-met genotype and individual variation in the brain response to amphetamine. Proc Natl Acad Sci USA 100:6186–6191.

McTavish SF, Cowen PJ, Sharp T (1999) Effect of a tyrosine-free amino acid mixture on regional brain catecholamine synthesis and release. Psychopharmacology (Berl) 141:182–188.

Mehta MA, Manes FF, Magnolfi G, Sahakian BJ, Robbins TW (2004) Impaired set-shifting and dissociable effects on tests of spatial working memory following the dopamine D2 receptor antagonist sulpiride in human volunteers. Psychopharmacology (Berl) 176:331–342.

Mehta MA, Gumaste D, Montgomery AJ, McTavish SF, Grasby PM (2005) The effects of acute tyrosine and phenylalanine depletion on spatial working memory and planning in healthy volunteers are predicted by changes in striatal dopamine levels. Psychopharmacology (Berl) 180:654–663.

Meyer-Lindenberg A, Straub RE, Lipska BK, Verchinski BA, Goldberg T, Callicott JH, Egan MF, Huffaker SS, Mattay VS, Kolachana B, Kleinman JE, Weinberger DR (2007) Genetic evidence implicating DARPP-32 in human frontostriatal structure, function, and cognition. J Clin Invest 117:672–682.

Middleton FA, Strick PL (2000) Basal ganglia output and cognition: evidence from anatomical, behavioral, and clinical studies. Brain Cogn 42:183–200.

Middleton FA, Strick PL (2002) Basal-ganglia "projections" to the prefrontal cortex of the primate. Cereb Cortex 12:926–935.

Mink JW (1996) The basal ganglia: focused selection and inhibition of competing motor programs. Prog Neurobiol 50:381–425.

Miyoshi E, Wietzikoski S, Camplessei M, Silveira R, Takahashi RN, Da Cunha C (2002) Impaired learning in a spatial working memory version and in a cued version of the water maze in rats with MPTP-induced mesencephalic dopaminergic lesions. Brain Res Bull 58:41–47.

Monchi O, Taylor JG, Dagher A (2000) A neural model of working memory processes in normal subjects, Parkinson's disease and schizophrenia for fMRI design and predictions. Neural Netw 13:953–973.

Monchi O, Petrides M, Petre V, Worsley K, Dagher A (2001) Wisconsin Card Sorting revisited: distinct neural circuits participating in different stages of the task identified by event-related fMRI. J Neurosci 21:7733–7741.

Monchi O, Petrides M, Doyon J, Postuma RB, Worsley K, Dagher A (2004) Neural bases of set-shifting deficits in Parkinson's disease. J Neurosci 24:702–710.

Monchi O, Petrides M, Mejia-Constain B, Strafella AP (2007) Cortical activity in Parkinson's disease during executive processing depends on striatal involvement. Brain 130:233–244.

Montgomery AJ, McTavish SF, Cowen PJ, Grasby PM (2003) Reduction of brain dopamine concentration with dietary tyrosine plus phenylalanine depletion: an [11C]raclopride PET study. Am J Psychiatry 160:1887–1889.

Nagano-Saito A, Washimi Y, Arahata Y, Kachi T, Lerch JP, Evans AC, Dagher A, Ito K (2005) Cerebral atrophy and its relation to cognitive impairment in Parkinson disease. Neurology 64:224–229.

Nathaniel-James DA, Frith CD (2002) The role of the dorsolateral prefrontal cortex: evidence from the effects of contextual constraint in a sentence completion task. NeuroImage 16:1094–1102.

Owen AM, James M, Leigh PN, Summers BA, Marsden CD, Quinn NP, Lange KW, Robbins TW (1992) Fronto-striatal cognitive deficits at different stages of Parkinson's disease. Brain 115:1727–1751.

Owen AM, Roberts AC, Hodges JR, Summers BA, Polkey CE, Robbins TW (1993) Contrasting mechanisms of impaired attentional set-shifting in patients with frontal lobe damage or Parkinson's disease. Brain 116:1159–1175.

Owen AM, Doyon J, Dagher A, Sadikot A, Evans AC (1998) Abnormal basal ganglia outflow in Parkinson's disease identified with PET. Implications for higher cortical functions. Brain 121:949–965.

Packard MG, Hirsh R, White NM (1989) Differential effects of fornix and caudate nucleus lesions on two radial maze tasks: evidence for multiple memory systems. J Neurosci 9:1465–1472.

Palmour RM, Ervin FR, Baker GB, Young SN (1998) An amino acid mixture deficient in phenylalanine and tyrosine reduces cerebrospinal fluid catecholamine metabolites and alcohol consumption in vervet monkeys. Psychopharmacology (Berl) 136:1–7.

Parent A (1990) Extrinsic connections of the basal ganglia. Trends Neurosci 13:254–258.

Pessiglione M, Guehl D, Rolland AS, Francois C, Hirsch EC, Feger J, Tremblay L (2005) Thalamic neuronal activity in dopamine-depleted primates: evidence for a loss of functional segregation within basal ganglia circuits. J Neurosci 25:1523–1531.

Poldrack RA, Clark J, Pare-Blagoev EJ, Shohamy D, Creso Moyano J, Myers C, Gluck MA (2001) Interactive memory systems in the human brain. Nature 414:546–550.

Postuma RB, Dagher A (2006) Basal ganglia functional connectivity based on a meta-analysis of 126 positron emission tomography and functional magnetic resonance imaging publications. Cereb Cortex 16:1508–1521.

Sawaguchi T, Goldman-Rakic PS (1994) The role of D1-dopamine receptor in working memory: local injections of dopamine antagonists into the prefrontal cortex of rhesus monkeys performing an oculomotor delayed-response task. J Neurophysiol 71:515–528.

Scatton B, Javoy-Agid F, Rouquier L, Dubois B, Agid Y (1983) Reduction of cortical dopamine, noradrenaline, serotonin and their metabolites in Parkinson's disease. Brain Res 275:321–328.

Shook SK, Franz EA, Higginson CI, Wheelock VL, Sigvardt KA (2005) Dopamine dependency of cognitive switching and response repetition effects in Parkinson's patients. Neuropsychologia 43:1990–1999.

Smith AD, Bolam JP (1990) The neural network of the basal ganglia as revealed by the study of synaptic connections of identified neurones. Trends Neurosci 13:259–265.

Sternberg S (1966) High-speed scanning in human memory. Science 153:652–654.

Taghzouti K, Louilot A, Herman JP, Le Moal M, Simon H (1985) Alternation behavior, spatial discrimination, and reversal disturbances following 6-hydroxydopamine lesions in the nucleus accumbens of the rat. Behav Neural Biol 44:354–363.

Taylor AE, Saint Cyr JA, Lang AE (1986) Frontal lobe dysfunction in Parkinson's disease. The cortical focus of neostriatal outflow. Brain 109:845–883.

Thesen S, Heid O, Mueller E, Schad LR (2000) Prospective acquisition correction for head motion with image-based tracking for real-time fMRI. Magn Reson Med 44:457–465.

Vogt BA, Finch DM, Olson CR (1992) Functional heterogeneity in cingulate cortex: the anterior executive and posterior evaluative regions. Cereb Cortex 2:435–443.

Williams D, Tijssen M, Van Bruggen G, Bosch A, Insola A, Di Lazzaro V, Mazzone P, Oliviero A, Quartarone A, Speelman H, Brown P (2002) Dopamine-dependent changes in the functional connectivity between basal ganglia and cerebral cortex in humans. Brain 125:1558–1569.

Williams-Gray CH, Hampshire A, Barker RA, Owen AM (2008) Attentional control in Parkinson's disease is dependent on COMT val158met genotype. Brain 131:397–408.

Worsley KJ (2005) Spatial smoothing of autocorrelations to control the degrees of freedom in fMRI analysis. NeuroImage 26:635–641.

Worsley KJ, Liao CH, Aston J, Petre V, Duncan GH, Morales F, Evans AC (2002) A general statistical analysis for fMRI data. NeuroImage 15:1–15.